A Comprehensive Qualitative and Quantitative Molecular Orbital Analysis of the Factors Governing the Dichotomy in the Dinorcaradiene ⇌ 1,6-Methano[10]Annulene System

Carlo Mealli,* Andrea Ienco, Earle B. Hoyt, Jr., and Robert W. Zoellner*

Abstract: The interconversion between the valence tautomers 1,6-methano[10]-annulene (**1**) and dinorcaradiene (**2**) was computationally investigated by qualitative extended Hückel molecular orbital methods (with CACAO visualization) and quantitative semiempirical and ab initio methods. The fundamental bonding interactions are described in terms of perturbation theory arguments for both tautomers, the influence of π-acceptor or π-donor substituents at the C11 position is rationalized, and bonding changes during the interconversion are monitored. The electronic molecular structural preferences can be modified by through-space interactions, and residual C1–C6 σ bonding r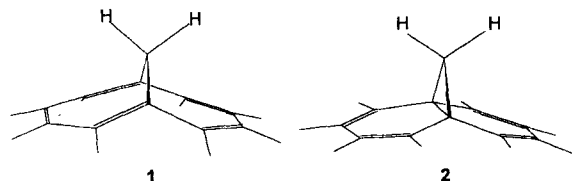emains even at the > 2.1 Å separations of the annulenic structures. Hitherto unprecedented calculations of the geometries of C11 homo-disubstituted derivatives of **1** and **2** have been carried out at semiempirical and ab initio levels to identify the more stable tautomer and find whether two stable minima may exist for each derivative. Searches at the AM1 level to determine transition-state structures for the interconversion of **1** to **2** and of their C11 homo-disubstituted derivatives are also reported.

Keywords
ab initio calculations · annulenes · semiempirical calculations
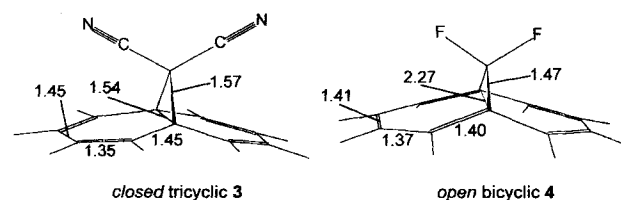
Introduction

Since Vogel and Roth's preparation[1] of 1,6-methano-[10]annulene (**1**) (formally bicyclo[4.4.1]undeca-1,3,5,7,9-pentaene) more than 30 years ago, many aspects of the chemistry of this interesting molecule and its valence tautomer dinorcaradiene (tricyclo[4.4.1.0^{1,6}]undeca-2,4,7,9-tetraene, **2**) have been discussed from theoretical,[2] synthetic,[3] and experimental[4] viewpoints. Recently, **1** has enjoyed a small resurgence of activity because of its use as the core for the preparation of amphiphilic systems[5] and as a ligand in metal complexes.[6]

1

2

[*] C. Mealli, A. Ienco
Istituto per lo Studio della Stereochimica ed Energetica dei Composti di Coordinazione dal Consiglio Nazionale delle Ricerche (ISSECC-CNR)
Via Jacopo Nardi 39, I-50132 Firenze (Italy)
Fax: Int. code +(55)247-8366
e-mail: mealli@cacao.issecc.fi.cnr.it

R. W. Zoellner, E. B. Hoyt, Jr.
Department of Chemistry, Northern Arizona University
Flagstaff, AZ 86011-5698 (USA)
Fax: Int. code +(520)523-8111
e-mail: robert.zoellner@nau.edu

The interconversion between **1** and **2** is analogous to the formation of adducts from fullerenes and carbenes.[7] For example, the addition of a carbene (or the synthetic equivalent of a nitrene) to the 6,6-fusion bond of C_{60} results in a cyclopropane-containing methanofullerene,[8] while an analogous addition to the 5,6-fusion bond of C_{60} forms a fulleroid, with concurrent cleavage of the 5,6-fusion bond.[9] The structural effects occurring when an inorganic handle is attached to C_{60} (e.g., a transition metal fragment[10] isolobal[11] with CH_2) have aroused our interest as well.[12]

Experimentally, the *open* bicyclic species **1** is favored over the *closed* tricyclic tautomer **2** by only 5.7 ± 2 kcal mol^{-1},[13] with a structure in agreement with the long C1–C6 separation of about 2.23 Å. The abundant X-ray data[14, 15] show that substituents at the apical C11 position can significantly alter the position of the equilibrium between the *open* bicyclic and *closed* tricyclic limits represented by the parent compounds **1** and **2**. As early as 1975, a geometric parameterization of the pericyclic 1,6 ring closure of **1** in terms of the available X-ray data had been carried out by Bürgi and Dunitz.[16, 17] However, while the 11,11-dicyano derivative **3**[15c] adopts the *closed* tricyclic dinor-

closed tricyclic **3**

open bicyclic **4**

caradiene form and the 11,11-difluoro derivative 4[14b] exhibits the *open* bicyclic annulene structure, the situation becomes less distinct with other apical substituents. In fact, the structures of the 11,11-dimethyl[15a] and 11-methyl-11-cyano derivatives[15b] are characterized by noncanonical C1–C6 bonds of about 1.8 Å in length. Importantly, none of the reported *open* or *closed* experimental structures deviate significantly from C_{2v} symmetry with respect to the core of the molecule when substituents are ignored.

Computational investigations[2] of the dinorcaradienes and the 1,6-methano[10]annulenes have increased modestly, in parallel with the number of experimental observations reported.[3, 4] Although some of the studies have been carried out at high levels of computational sophistication, including unrestricted Hartree–Fock (UHF) methods at the semiempirical AM1 level[7] and Møller–Plesset perturbation theory methods at the ab initio level,[2b] some of the computationally optimized structures are questionable when compared to experiment. For example, some models optimize to an *open* structure with a long C1–C6 distance, similar to 1, but are characterized by inequivalent lateral six-membered rings with overall C_s rather than C_{2v} symmetry.[3a] Thus, one goal of the present discussion is to calculate systematically, for the first time, the structures of a number of derivatives of both 1 and 2 with different substituents at the apical carbon atom C11. Furthermore, to the best of our knowledge, no comprehensive overview of the electronic and steric factors affecting the tautomerism between 1 and 2 has been presented previously.

All of our discussions address both qualitative and quantitative molecular orbital (MO) approaches. The computational methods we employ are extended Hückel (EHMO),[18] semiempirical RHF-AM1,[19] and higher-level ab initio RHF-3-21 G(*) and RHF-6-31 G* methods,[20, 21] the latter using SPARTAN.[22] We have also used the SPARTAN suite of programs to investigate the AM1 level structures of the transition states (TSs) during the interconversions of 1 and 2 and their derivatives.

Our description of the system begins with the basic chemical bonding in naphthalene, proceeds with the addition of a methylene handle to the central C–C bond of naphthalene, and then follows the evolution of the system toward either the dinorcaradienic or the 1,6-methano[10]annulenic structure. A qualitative picture of this process at the EHMO level can be quickly attained with the graphical interface package CACAO.[23] Visualization of the frontier molecular orbitals along the interconversion pathway allows direct evaluation of the consistency between experimental and computational data in terms of simple perturbation theory arguments.[24] In the absence of such an interpretational tool, a chemist's intuition is limited to the valence bond (VB) formalism intrinsic in the drawings of 1 and 2.

Results and Discussion

Parameters affecting the interconversion between limiting geometries: Initially, it is important to identify the geometric structural parameters that define the interconversion between the dinorcaradiene and the 1,6-methano[10]annulene tautomers. We have used the structures of the 11,11-dicyano[15c] and the

11,11-difluoro derivatives[14b] as definitive extremes in this regard.

The Cambridge Structural Database[25] contains about 30 X-ray structures of derivatives of 1 and 2 having different substituents at the apical C11 carbon atom as well as at other positions. In most cases, the accuracy of the experimental results was sufficient to reliably determine the positions of the hydrogen atoms in the structures. Such a determination is crucial if an accurate picture of the molecular stereochemistries and a parameterization of the interconversion pathway is to be developed.

Essentially, 1 and 2 can be described as containing a CR_2 handle attached to the 6,6-ring-fusion edge (by analogy to C_{60} literature) of naphthalene. When R = CN, a cyclopropane-like bonding network arises, as is clear in the end-on view I. It is well established that π-acceptor substituents on C1 of a cyclopropane[26] cause the C2–C3 bond to shorten, while π-donor groups lead to bond lengthening. (A qualitative MO explanation of this effect has been reported.[27]) In no case, however, can substituents alone cause a cyclopropane system to undergo ring-opening; cyclopropane ring-opening occurs homolytically.[28]

I   II
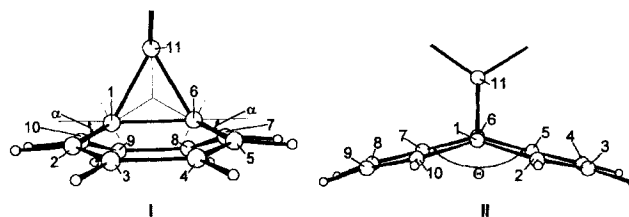
The side-on view II clearly demonstrates that the lateral C_6 rings maintain their individual planarity, but that each has rotated from the plane of the original naphthalene system by about 15°, corresponding to a *bookfolding* dihedral angle Θ of about 150°. In the X-ray structure of the *closed* tricyclic 11,11-dicyano derivative,[15c] $\Theta = 151.15°$; our calculations result in $\Theta = 143.39°$ (AM1), 146.54° (3-21 G*) and 144.83° (6-31 G*). The dihedral angle Θ defines the major structural rearrangement parameter during the attachment of a CR_2 handle to naphthalene.

The dihedral angle Θ also determines the tilting angle α of the plane C2-C1-C10 (and its equivalent) with respect to the C1–C6 vector. For $\Theta = 151°$, α is about 24°. For comparison, in cyclopropane the structurally required orientation of each CH_2 moiety must correspond to $\alpha = 30°$ with respect to either of its adjacent C–C vectors. Accordingly, all of the methylene radial orbitals in cyclopropane (III) point exactly to the center of the C_3 triangle. There are also in-plane tangential orbitals (IV) which, together with the radial orbitals, form the C_3 σ-bonding network.

radial p_σ tangential p_σ

III   IV
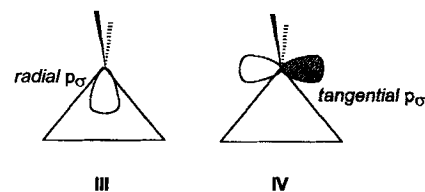
It is instructive to recall the concept of σ aromaticity for such a network (see **V**, Figure 1).[29, 30] In the D_{3h} symmetry of cyclopropane, the radial (**III**) and tangential (**IV**) orbitals give rise to the Hückel aromatic MO pattern of three filled and bonding MOs well separated from the higher energy and empty antibonding MOs. This simplified MO picture will become useful during the discussion (vide infra) of the bond-breaking/bond-making aspects within the cyclopropane unit of the dinorcaradiene ⇌ 1,6-methano[10]annulene system.
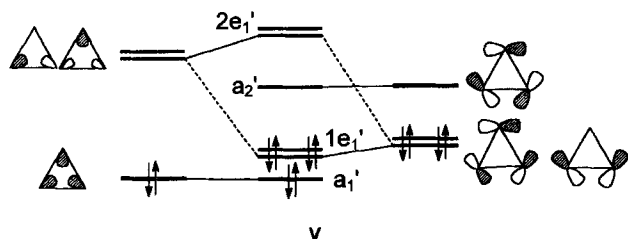

V

Figure 1. Methylene radial (**III**) and in-plane tangential orbitals (**IV**) which together form the C_3 σ-bonding network.

In **VI**, the structure of 11,11-difluoromethano[10]-annulene[14b] (**4**) is shown in the same end-on view as was used in **I** for **3**. The elongation of the C1−C6 vector is evident, and a larger α angle of about 51° is also observed (the C1-C11-C6 angle is about 98°). Because of the magnitude of α, the radial orbitals of the two methylene-like units (defined by the triad C2-C1-C10 and its symmetry equivalent) are now redirected from the center of the triangle toward C11. From the orthogonal viewpoint **VII**, it is evident that the planarity of the two C_6 rings is lost: each ring is now folded by 20° ($\Phi = 160°$) about the C2−C5 and C7−C10 vectors. In addition, the C−H bonds of the atoms of these vectors are twisted downwards so as to become nearly coplanar with the C2-C1-C10 plane or its symmetry equivalent (see **VI**). The internal C-C-C angles of the C_6 rings (γ and δ in **VIII**) have opened significantly from 120° in the

VI   **VII**
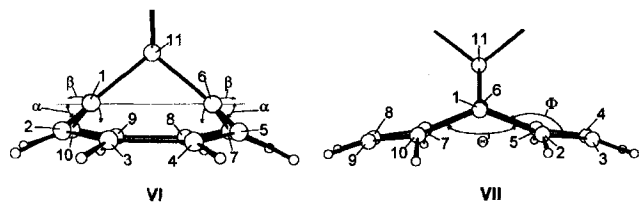
closed tricyclic to as much as about 128° in the open bicyclic derivative. (Our computational results at semiempirical and ab initio levels of theory are consistent with these structural parameters from extended Hückel calculations.)

By reference to a simple molecular modeling kit, the interconversion between **1** and **2** could be shown to potentially occur by a combination of torsions at various C−C bonds. A reasonable pathway could be mimicked by using a restricted number of parameters and adopting the strategy illustrated in **VIII**. This

VIII
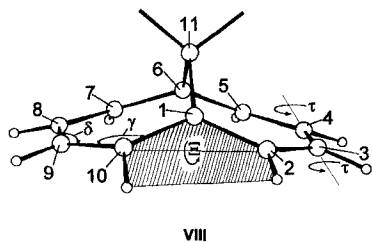
parameterization was further elucidated by our TS structural investigations (vide infra). Because C_{2v} symmetry is maintained throughout the interconversion pathway, the movements of atoms or groups of atoms are mirrored by their symmetry equivalents during the interconversion.

Beginning with the closed tricyclic structure fixed as a $\Theta = 150°$ bookfolded naphthalene moiety with a CH_2 handle, the tetraatomic unit HC3−C4H is rotated by a small angle ($\tau \leq 4°$) about the C3−C4 vector. Simultaneously, the atoms defining the plane H-C2-C1-C10-H are rotated about the C2−C10 vector to an angle Ξ of up to 20°. In this manner, a simultaneous double envelope-opening process significantly elongates the C1−C6 distance. This parameter could not attain the value of about 2.2 Å observed in the open bicyclic structures unless allowances were made to also increase the γ and δ angles to their experimental values, which are significantly larger than 120°.[31]

An MO description of the chemical bonding and its evolution during the closed-open interconversion:

The closed tricyclic dinorcaradiene tautomer: An in-depth knowledge of π delocalization in naphthalene is fundamental to the evaluation of the effects of adding a methylene handle to the 6,6-fusion edge of the molecule and, hence, to the compatibility of a central cyclopropane unit with the two lateral portions of the naphthalene system. As shown in Figure 2, naphthalene can be conveniently constructed in terms of more elementary com-

Figure 2. Schematic description of the filled naphthalene π MOs in terms of their basic components (two lateral butadienic moieties plus a central ethylenic C_2 unit).

ponents: the in-phase (i.p.) and out-of-phase (o.o.p.) bonding and antibonding π levels of two butadienic fragments and the π and π* levels of a central ethylenic unit.

The five filled naphthalene π MOs are primarily symmetry combinations of the bonding MOs of the elementary components: two from each lateral butadienic fragment and one from the central ethylenic moiety. However, the filled $1b_{3g}$ MO also has a large ethylenic π* contribution, which causes the 6,6-fusion edge of naphthalene to elongate. The π* character in both the filled ($1b_{3g}$) and the empty ($2b_{3g}$) MOs will ultimately become a critical factor governing the *closed* tricyclic ⇌ *open* bicyclic structural dichotomy (vide infra).

In order to establish a qualitative reference point, a generic methylene fragment, characterized by a radial p_σ (**III**) and a tangential p (**IV**) orbital, is allowed to interact with naphthalene (D_{2h} symmetry), as shown schematically in **IX** (Figure 3). The
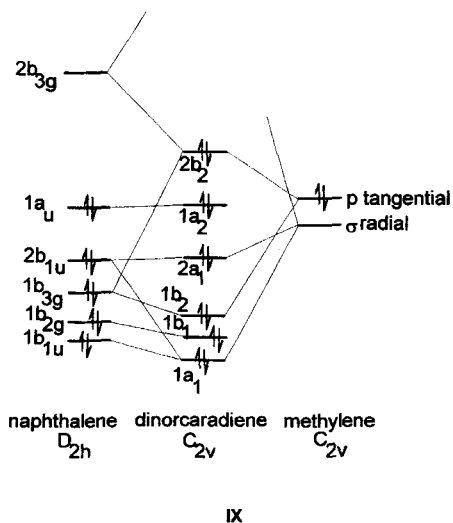

Figure 3. Interaction of a generic methylene fragment characterized by a radial p_σ and a tangential p orbital with naphthalene (D_{2h} symmetry).

σ-bonding component of the incipient cyclopropane moiety initially results from the interaction of the low-lying $1b_{1u}$ and $2b_{1u}$ MOs ($1a_1$ and $2a_1$ in C_{2v} symmetry, respectively) with the methylene p_σ radial orbital. When bookfolding occurs, a σ-bonding MO of the 6,6-fusion edge also becomes involved in the orbital mixing process so as to produce a cyclopropane-like a_1' bonding combination similar to that shown in **V**.

Although slightly higher in energy than the p_σ radial orbital, the p tangential orbital can be formally assigned the methylene electrons, as only this orbital is capable of donating electron density into the empty naphthalene $2b_{3g}$ level. The situation is complicated by the participation of the lower-lying $1b_{3g}$ naphthalene level because of its implicit ethylenic π* character. The overall three-center, four-electron interaction would cause a significant destabilization of the $2b_2$ HOMO of the system if the naphthalene moiety remained planar. However, bookfolding can stabilize the $2b_2$ HOMO and, therefore, the whole system. Such stabilization is evident from a Walsh diagram for the 11,11-dicyano derivative (not shown) which indicates that, at the EHMO level, the system gains about 2.6 eV during bookfolding. Further, a minimum in energy is attained at about $\Theta = 150°$, in agreement with the experimental structural data.

The relative energies of the CR_2 orbitals obviously must depend significantly on the nature of the substituents. When R = CN, the π* orbitals of the cyano groups cooperatively lower the energy of the p orbital on the central carbon, while when R = F, the filled fluorine p orbitals cause the p orbital to be raised in energy by as much as 2 eV (compare **X** and **XI**) relative
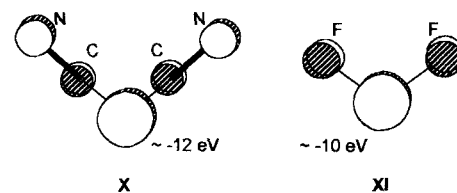

to the dicyano system. When the energy difference with respect to $2b_{3g}$ and the CR_2 orbitals diminishes, the donor–acceptor interaction is favored, and because the energy difference with respect to the filled $1b_{3g}$ simultaneously increases, the effect of the destabilizing three-center, four-electron repulsion is concurrently lessened.

More efficient electron donation from the carbon p orbital into the $2b_{3g}$ orbital, which is π antibonding at the 6,6-ring-fusion bond of naphthalene, also forces the bond to lengthen. The analogous substituent effect in cyclopropanes has been explained similarly.[27] In the present dinorcaradiene ⇌ 1,6-methano[10]annulene system, however, the C1–C6 distance can become longer than 2.1 Å. Below, we discuss in detail the question of whether this length change implies bond stretching or bond cleavage. At this point, however, the above arguments suggest that the difluoro derivative is one of the best candidates for bond cleavage. On the other hand, our ab initio calculations suggest that the *closed* tautomer of the difluoro derivative is realistic as well (vide infra).

Two important aspects related to the nature of the substituents should be mentioned at this point. First, the 11,11-dichloro derivative, whose structure has not been determined, is expected to favor the *open* structure even more strongly than the difluoro derivative. In fact, the filled chlorine p orbitals force the C11 carbon p orbital to a higher energy than was seen in **XI**. In contrast, our EHMO, semiempirical, and ab initio calculations uniformly and distinctly favor the *closed* structure for the dichloro derivative. Another peculiar case is that of the 11,11-dimethyl derivative, whose methyl substituents can be attributed some π-donor capability. The compound has been experimentally shown to have an intermediate C1–C6 bond length of about 1.8 Å which is neither truly *open* nor truly *closed*. In these cases, structural preferences are in apparent conflict with the electronic effects outlined above. In the next section, the competing effect of intramolecular steric hindrance in determining the most stable tautomer will be analyzed.

Presently, we shall continue to use the qualitative EHMO picture to better understand the cause of the C1–C6 elongation. The process of bookfolding provides an approximate energy gain of 1.8 eV for the difluoro derivative compared to a gain of 2.6 eV for the dicyano derivative. A visual comparison (see **XII**) of the two HOMOs ($2b_2$ at $\Theta = 30°$) not only accounts for the energy difference but also for the preference of the difluoro derivative to open.
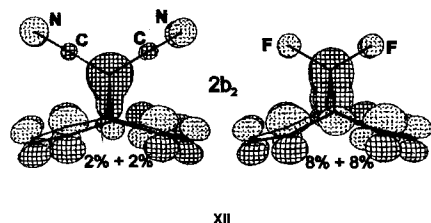
XII

The contribution of orbitals on C1 and C6 to these MOs is significantly smaller for the dicyano derivative (2% vs. 8%), because the three-orbital interaction involving the carbon p and the two naphthalene b_{3g} levels (see Figures 2 and 3) forces mixing between $2b_{3g}$ and $1b_{3g}$. Perturbation theory indicates that while π^* antibonding between the central ethylenic unit and the butadienic wings is almost eliminated in the dicyano derivative, the difluoro derivative is still significantly destabilized. Moreover, a *through-space* interaction between the C11 p orbital and the butadienic wings can also be observed in **XII**. By increasing the degree of bookfolding, the through-space repulsion is reduced and the HOMO is stabilized.

It is instructive to compare the three b_2 MOs in **IX** with the π system of the allyl anion, in which a typical four-electron, three-center interaction occurs. In the anion (**XIII**), electronic repulsions are minimized because the π_{nb} MO has a node at the central carbon atom. Although never perfectly achieved, a similar situation occurs here, as illustrated in **XIV**. The filled $2b_2$ level (HOMO) accumulates electron density on both the apical C11 and on the butadienic wings of the molecule because (ideally) a node exists at the C1 and C6 atoms. The dashed-line partitioning in **XIV** highlights this aspect.
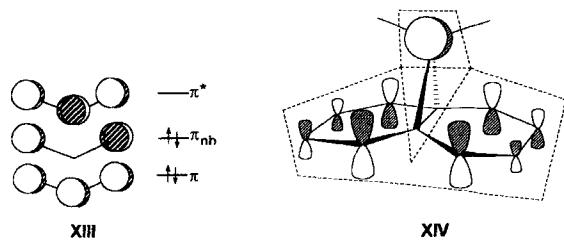
XIII   **XIV**

The $1b_2$ MO (the equivalent of the allyl π orbital) is overall bonding between the components in **XIV**. Because of its highly delocalized nature, the separation into different components is an oversimplification. However, $1b_2$ can be considered to be responsible for one of the three σ bonds needed for the cyclopropane network. Indeed, disregarding the contribution from the lateral butadienic wings, the orbital resembles the left-hand $1e'_1$ level previously illustrated in **V**. The right-hand $1e'_1$ orbital is related to the original naphthalene $2b_{1u}$ level ($2a_1$ in **IX**) because, during the bookfolding process, the p orbitals of C1 and C6 reorient toward each other. Finally, the cyclopropane a'_1 level is formed from a C1–C6 σ-bonding MO (not shown) which partially mixes with the filled naphthalene $1b_{1u}$ and $2b_{1u}$ MOs of Figure 2.

The remaining four π-electron pairs of the naphthalene fragment preferentially localize on the lateral butadienic wings.[32] Aside from the contribution of $1b_2$, the π bonding between the wings and C1 and C6 is small. As a whole, the simplified MO description underscores and extends the VB description in **3**.

From the above analysis it is also evident that additional, primarily repulsive, residual π interactions may still exist between the central cyclopropane moiety and the lateral butadienic wings. The HOMOs in **XII** indirectly support this position. To eliminate these sources of destabilization, the system can rearrange to produce an alternative electronic distribution.

The 1,6-methano[10]annulene tautomer: Experimentally, each C11-substituted derivative exists either as the dinorcaradiene or the 1,6-methano[10]annulene structure. (To our knowledge, the only substantiated equilibrium between the two forms is that of the parent compounds containing an apical CH_2 group.[7, 13]) However, both semiempirical and ab initio calculations find structural minima for both tautomers in many cases. Now, however, we shall proceed with our illustration of the qualitative picture with the 1,6-methano[10]annulene tautomer and the geometric interconversion to it from dinorcaradiene.

Figure 4 illustrates the behavior of selected frontier MOs of the difluoro derivative during its evolution from the *closed* to the *open* structure by means of the parameters previously established for this interconversion (**VI–VIII**). The essential feature
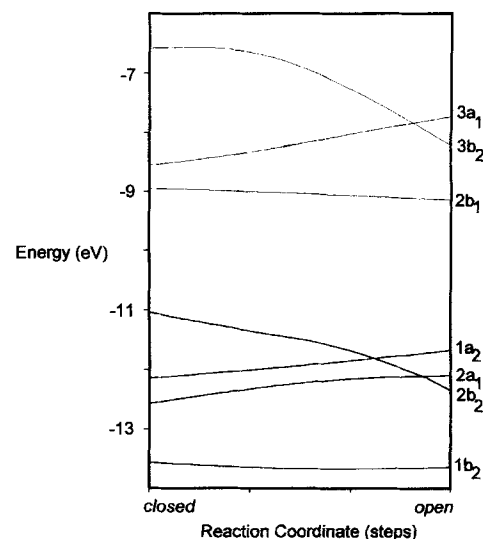

Figure 4. A Walsh diagram showing the evolution of selected frontier MOs during the dinorcaradiene $\rightleftharpoons$ 1,6-methano[10]annulene interconversion for the 11,11-difluoro derivative.

of this figure is that the HOMO of the *closed* dinorcaradiene (the $2b_2$ level) becomes significantly stabilized and, as the *open* structure is attained, the $2b_2$ level crosses the two lower energy $1a_2$ and $2a_1$ levels, which are themselves somewhat destabilized. At the EHMO level, the net energy gain is about 17 kcal mol^{-1} in favor of the 11,11-difluoro-1,6-methano[10]annulene.

The trends in this Walsh diagram are confirmed by the order of the filled frontier MOs in the ab initio 6-31 G* calculations for the two structural minima. The calculated ordering for the 11,11-difluorodinorcaradiene tautomer in descending energy is $2b_2$, $1a_2$ and $2a_1$, while for the 11,11-difluoro-1,6-methano[10]-annulene tautomer, $2b_2$ has become the third-highest filled level, with an increase in stabilization of about 1.5 eV. During the interconversion, interlevel crossing must occur, and from an MO viewpoint this indicates the possible existence of two structural minima.
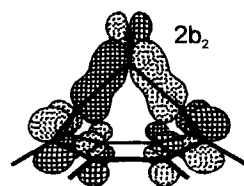
Visual analysis of the MOs provides a reasonable explanation for the change of the HOMO from $2b_2$ to $1a_2$. As shown in **XV**, the direction of the σ hybrid orbitals on C1 and C6 is most affected by the interconversion process. In naphthalene, these orbitals point directly toward each other and in the *closed* tautomer they point toward the center of the cyclopropane moiety,
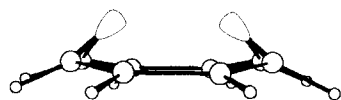
but in the *open* structure the orbitals diverge even further and point directly at C11. This continuing divergence causes the σ* combination of the hybrids in **XV** to descend steeply in energy and mix with other b_2 levels (in particular the ethylenic π* orbital, formerly $2b_{3g}$ in Figure 2). Eventually four of the b_2 levels, rather than the three which appeared in **IX**, must be considered.

XV

Although something of an oversimplification, the situation can be described as follows: The MOs $2b_2$ and $4b_2$ are the σ and σ* combinations relative to the bonding between the hybrids **XV** and the C11 p orbital. Recall that in the *closed* difluoro derivative, $2b_2$ (see the right-hand part of **XII**) was affected by an unfavorable π* interaction between the central ethylenic

moiety and the butadienic wings. In the *open* tautomer, the $2b_2$ MO (**XVI**) clearly shows residual π* features in addition to the prevailing σ-bonding character. The roles of the $1b_2$ and $3b_2$ orbitals remain to be clarified.

2b₂

XVI

To comply with the VB structure **4**, none of the original ten naphthalene π electrons should be used for bonding between C1 and C6. Thus, more π interaction is expected at the bonds connecting these atoms to the butadienic wings (which is partially confirmed by a modest increase in the overlap populations for these bonds). However, C1 and C6 are in nearly ideal sp² environments. Their orthonormal p_π orbitals are far from parallel with the p_π orbitals of the butadienic wings (the skew angle between them can be as large as 45°). Thus π bonding between them must be attenuated. The role of the filled $2a_1$ and the empty $3b_2$ MOs (**XVII** and **XVIII**, respectively) becomes critical in the evaluation of the overall bonding picture.

2a₁ **3b₂**
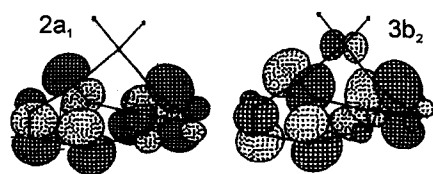
XVII **XVIII**

Each of these orbitals exhibits a significant (ca. 60%) contribution from the p_π orbitals on C1 and C6, but their respective π and π* interaction with the lateral butadienic π systems is modest. Instead, these levels are characterized by prevailing σ

and σ* characters that do not exclude direct C1–C6 interactions even when the separation is long.

To further elucidate the situation, we refer back to cyclopropane (see **V**). Assume that one C-C-C angle of cyclopropane opens and the carbon atoms of the two separating CH_2 groups become planar. The relative Walsh diagram is illustrated in Figure 5 (**XIX**). The loss of bonding character in the $2a_1$ combina-

C-C-C opening
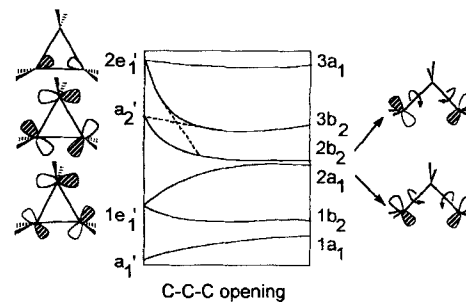
XIX

Figure 5. Walsh diagram for opening of one C-C-C angle of cyclopropane.

tion (originally a member of the degenerate $1e'_1$ level) and the loss of antibonding character in the $2b_2$ combination (in which one steeply descending member of the degenerate $2e'_1$ level mixes with the lower a'_2 MO) results in the quasi-convergence of these two frontier levels.
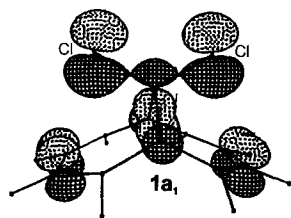
It is well-known that opening of cyclopropane occurs homolytically,[28] and a rigorous quantitative discussion of this problem is not within the scope of this article. However, the following qualitative arguments are meaningful: In Figure 5, the acquired degeneracy of the $2b_2$ and $2a_1$ levels on ring opening and their equal orbital contributions from the separating carbon atoms imply a smooth transformation from a singlet to a triplet ground state, leading eventually to the formation of a diradical. The rotation of the terminal CH_2 groups about the C–C bonds, which prevents the electrons from re-pairing, provides further stability to the diradical. Similar MO features have previously been pointed out for organometallic systems in which metal–carbon bond homolysis occurs.[33]

The diagram in Figure 4, for the dinorcaradiene ⇌ 1,6-methano[10]annulene rearrangement, exhibits similarities, but also major differences, in comparison with Figure 5. The i.p. and the o.o.p. combinations of the p_π orbitals of C1 and C6 are stabilized and destabilized, respectively, during the interconversion, and they would be expected to converge. However, this convergence is prevented by the interactions with the π systems of the two lateral butadienic wings. The two levels remain well separated: In no case does the gap between the $3b_2$ and $2a_1$ levels become less than 3 eV. Moreover, since these levels cannot even become adjacent (the $1a_2$ and $2b_1$ π levels always remain at intermediate energies), the possibility of an electron transition to form a triplet ground state can be excluded. Given the MO picture, as well as the rigidity of the system, there is little possibility that the dinorcaradiene ⇌ 1,6-methano[10]annulene tautomerism proceeds via a diradical.

As stated above, the coexistence of a filled $2a_1$ and an empty $3b_2$ MO (**XVII** and **XVIII**) suggests a residual σ bond at C1–C6

even for long experimental separations. This σ bond is in competition with π bonding to the lateral butadienic wings. The π bonding would become 100% effective if the empty $3b_2$ level had solely π^* character and the filled $1b_2$ was its π-bonding partner. In other words, the latter description, which is simply the viewpoint suggested by the VB formula **4**, is not strongly supported by the MO analysis. In fact, the MO topology, the electronic distribution, and the C1–C6 overlap population (never smaller than 0.1) indicates that the σ bond between C1 and C6, although steadily weakened during the interconversion process, is never completely eliminated.

In concluding this section, we address in more detail some of the intriguing aspects of the tautomerism of the dichloro and dimethyl derivatives. As mentioned earlier, the dichloro derivative is more stable at the *closed* minimum. Indeed, our 6-31 G* ab initio calculations could not even find a stable minimum for the *open* structure. According to our interpretation of the interconversion, the chlorine p orbitals of the CCl_2 group, which are higher in energy than the p orbitals of fluorine in CF_2, should trigger the opening of the central C1–C6 bond even more readily than does CF_2. However, a Walsh diagram (not shown, but see **XX**) similar to that in Figure 4 provides a satisfactory answer for this incongruity: For the dichloro derivative, the three highest filled MOs behave similarly to those in the diagram for CF_2, but the energetics of the whole system are strongly influenced by a sharply rising $1a_1$ level.

XX

Structure **XX** confirms the σ bonding character of the orbital at the C1–C6 bond. However, this orbital is destabilized because of repulsive interactions between the in-plane lone pairs of the two chlorine atoms and the π system of the butadienic wings, to which the lone pairs are directed. This interaction prevents the upward twist of the wings (the Φ angle, see **VII**). Thus, in the case of the 11,11-dichloro derivative, intramolecular steric hindrance becomes the governing factor in favor of the *closed* structure. Perhaps for analogous reasons, as has been shown computationally, the CBr_2 group attached to a 6,6-fusion edge of C_{60} is not accompanied by a significant lengthening of that edge.[34]

An accurate X-ray crystallographic study[15a] of the dimethyl derivative has shown that the C1–C6 bond has an unusual length: 1.780(7) Å and 1.836(7) Å for the two molecules in the asymmetric unit. In this case, again, only the *closed* structure with a normal C1–C6 bond length results from our 6-31 G* ab initio calculations. Somewhat surprisingly, the corresponding EHMO Walsh diagram exhibits a minimum in total energy that corresponds closely to the experimental structure. Referring to the interconversion pathway defined by the coordinates in **VI**, **VII**, and **VIII**, this minimum is about midway along the pathway, whereby the *closed* and *open* structures are about 0.2 and 0.4 eV higher in energy, respectively. Apparently, an exceptionally delicate balance of steric and electronic effects occurs here. The stabilization of the $2b_2$ level on opening (see Figure 4) is effectively counterbalanced by the destabilization of the $2a_1$ and

$1a_2$ frontier levels, as well as that of the lower $1a_1$ level (somewhat similar to **XX**).

Semiempirical and ab initio calculations: The results of ab initio calculations should be generally regarded as the standard for a reliable study of the tautomerism of the organic species we describe here. However, correlating our results with a qualitative MO analysis has allowed us to focus on the fundamental aspects of the interconversion process. Now the qualitative MO picture can also be used as a convenient guide for the analysis of the results at higher levels of theory.

In general, the calculated heats of formation and electronic energies (Table 1) are in agreement with experimental data for the more stable tautomer of each known compound. With a few exceptions, the calculations also show that a second, local minimum exists which corresponds to the alternative tautomer. Since the experimental structures exhibit C_{2v} or pseudo-C_{2v} symmetry (where pseudo means that the core of the molecule is
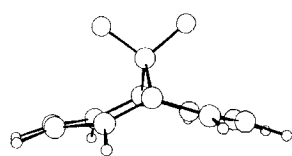
Table 1. Energies of selected 11,11-disubstituted dinorcaradienes and 1,6-methano-[10]annulenes calculated at semiempirical and ab initio levels of theory [a].

Compound [b]	Heat of formation, AM 1 (kcal mol^{-1}) [c]	Energy, 3-21 G$^{(*)}$ (Hartree) [c]	Energy 6-31 G* (Hartree) [c]
11,11-(C≡N)$_2$ (3)	**162.9574**	**− 602.352722**	**− 605.738895**
11,11-(C≡N)$_2$	163.2338	− 602.338051 [d]	− 605.716215
ΔE	0.276	9.21	14.2
11,11-(F)$_2$	1.1745	− 616.573320	− 619.987609
11,11-(F)$_2$ (4)	**− 0.1640**	**− 616.583419 [d]**	**− 619.990946**
ΔE	− 1.34	− 6.34	− 2.09
11,11-(H)$_2$ (2)	88.1109	− 419.927778	− 422.286827
11,11-(H)$_2$ (1)	**81.0626**	**− 419.934821 [d]**	**− 422.287099**
ΔE	− 7.05	− 4.40	− 0.17
11,11-(CH$_3$)$_2$	**82.4881**	**− 497.564233**	**− 500.349723**
11,11-(CH$_3$)$_2$	86.4170	− 497.557564 [e]	
ΔE	3.93	4.18	one minimum
11,11-(CH=CH$_2$)$_2$	**134.8373**	**− 572.821693**	**− 576.031248**
11,11-(CH=CH$_2$)$_2$	137.1420	− 572.813265 [f]	
ΔE	2.30	5.29	one minimum
11,11-(C≡CH)$_2$	**210.6226**	**− 570.420325**	**− 573.616889**
11,11-(C≡CH)$_2$	213.2654	− 570.407880 [d]	
ΔE	2.64	7.81	one minimum
11,11-(Cl)$_2$	**84.2797**	**− 1333.551438**	**− 1340.064379**
11,11-(Cl)$_2$	84.8590	− 1333.542595 [d]	
ΔE	0.579	5.55	one minimum
11,11-(NO$_2$)$_2$	**115.5994**	− 824.462249	**− 829.187373**
11,11-(NO$_2$)$_2$	116.9833	− 824.462426 [d]	− 829.177874
ΔE	1.38	− 0.111	5.96
11,11-(SiH$_3$)$_2$	**103.2966**	**− 997.217870**	**− 1002.430619**
11,11-(SiH$_3$)$_2$	106.7941	− 997.202386 [e]	− 1002.408151
ΔE	3.50	9.72	14.10

[a] The information for each compound is provided in two lines, the first referring to the *closed* dinorcaradienic structure and the second to the *open* annulenic structure. The designation of the experimentally stable structure, when known, and the calculated lower energy structure for a given method are printed in **boldface** type. [b] The energy difference, defined as $\Delta E = E(\text{open}) - E(\text{closed})$, for a given calculational method is reported in kcal mol^{-1} (1 Hartree = 627.5095 kcal mol^{-1}) and has been arbitrarily reported to three significant digits. [c] Unless otherwise indicated, all results were optimized without the imposition of any symmetry constraints. The energy differences between the ab initio optimizations with and without symmetry constraints were generally small (less than 1.5 kcal mol^{-1}), and appeared to decrease with increasing computational level. Semiempirical heats of formation and ab initio energies are arbitrarily reported to four decimal places for the former and to six decimal places for the latter. [d] Structure optimized by imposing C_{2v} symmetry constraints. [e] Structure optimized by imposing C_s symmetry constraints. [f] Structure optimized by imposing C_2 symmetry constraints.

of C_{2v} symmetry, but that some substituents, such as methyl or vinyl, may force an overall lowering of that symmetry), all of the calculations were performed under the appropriate symmetry constraints. Although these results appeared generally reasonable, we have occasionally observed that removal of the symmetry constraints provided otherwise unobtainable convergence (e.g., for the closed dicyano derivative). Because of the larger number of parameters involved in the absence of symmetry constraints, a slightly lower energy (always <2 kcal mol^{-1} at ab initio levels) was also obtained.

Such a difference is of little concern for the *closed* structures, as they remain very close to C_{2v} symmetry even in the absence of symmetry constraints. However, the *open* structures, optimized without the imposition of symmetry constraints, exhibit conformations for the two lateral C_6 moieties which are significantly asymmetric in comparison to each other, even at the 6-31G* level of theory. A typical example is provided by the calculated C_1 structure of the *open* difluoro derivative, shown in **XXI**. Note that the right-hand C_6 moiety mantains the planarity exhibited by both the experimental and computational *closed* structures, while the left-hand C_6 moiety is characterized by a Φ angle (see **VII**) of about 20°.

XXI

Although this moiety may superficially resemble the experimental structures for the *open* derivatives, such an angle is larger than that experimentally observed for any *open* structure.

Other authors[2a] have pointed out similar conformations in the calculated structures of the parent compound **1**, and did not exclude the possibility that a structure such as **XXI** could be an artifact of the computational method. There could also be an element of homoaromaticity[35] in such a structure, since the right-hand unit contains 6 π electrons but an open bond, while the left-hand unit adopts the features of a butadienic moiety with 4 π electrons.

There are well-documented circumstances in the chemical literature in which a molecule that could in principle adopt a higher symmetry structure is forced by a particular electronic configuration to distort to a lower symmetry conformation. Common examples are provided by cyclic antiaromatic molecules[36] in which Jahn–Teller effects are active.[37] Thus, cyclobutadiene is rectangular rather than square[38] and neutral cyclooctatetraene is not octagonal, but tub-shaped.[39] Analogous electronic requirements force the C_{24} fullerene to prefer D_6 rather than D_{6d} symmetry.[40] In each of these cases, the Jahn–Teller effect removes the degeneracy of the highest occupied levels by causing a molecular distortion to a lower-symmetry, more stable structure.

We have no computational indication that such an electronic argument can be applied to our system. In fact, all of the systems we have investigated are singlets with large HOMO–LUMO gaps. In any event, since our systems are of C_{2v} symmetry, and such a classification has no degenerate irreproducible representations, a Jahn–Teller effect per se cannot occur. Accordingly, our discussion is based on the C_{2v} symmetry tautomers and their

interconversion is assumed to occur via a C_{2v} pathway throughout.

The first result of note in Table 1 is that the computationally most stable tautomers are the *closed* for the dicyano and the *open* for the difluoro derivative. These species also have two of the highest interconversion activation energies (see Table 2).

Table 2. Semiempirical AM 1 calculations for the transition state structures and the activation energies and Boltzmann distributions of the ground-state molecules of selected 11,11-disubstituted dinorcaradienes and 1,6-methano[10]annulenes [a].

Compound	Heat of formation of transition state (kcal mol^{-1}) [b]	Activation energy E_a (kcal mol^{-1})	Calculated Boltzmann distribution
11,11-(C≡N)₂ (3)	173.1822	**10.2248**	**60.03%**
11,11-(C≡N)₂		9.9484	39.97%
11,11-(F)₂	10.2200	9.0455	8.48%
11,11-(F)₂ (4)		**10.3840**	**91.52%**
11,11-(H)₂ (2)	93.1975	5.0866	0.01%
11,11-(H)₂ (1)		**12.1349**	**99.99%**
11,11-(CH₃)₂	91.9540	**9.4659**	**99.93%**
11,11-(CH₃)₂		5.5370	0.07%
11,11-(CH=CH₂)₂	144.4998	**9.6625**	**98.67%**
11,11-(CH=CH₂)₂		7.3578	1.33%
11,11-(C≡CH)₂	221.2880	**10.6654**	**99.23%**
11,11-(C≡CH)₂		8.0226	0.77%
11,11-(Cl)₂	93.5838	**9.3041**	**93.58%**
11,11-(Cl)₂		8.7248	6.42%
11,11-(NO₂)₂	126.0251	**10.4257**	**92.19%**
11,11-(NO₂)₂		9.0418	7.81%
11,11-(SiH₃)₂	113.9985	**10.7019**	**99.84%**
11,11-(SiH₃)₂		7.2044	0.16%

[a] The information concerning the activation energy E_a for each compound is provided in two lines, the first referring to the *closed* dinorcaradienic structure and the second to the *open* annulenic structure. The designation of the experimentally stable structure, when known, and the results for the calculated lower energy structure at the semiempirical AM 1 level are printed in **boldface** type. Semiempirical heats of formation and ab initio energies have been arbitrarily reported to four decimal places for the former and to six decimal places for the latter. [b] All transition state results were optimized without the imposition of any symmetry constraints. However, the resulting transition state structures closely approximated C_{2v} symmetry.

The rationale previously proposed for these preferences in terms of π-acceptor and π-donor capabilities of the substituents is confirmed by these results. Moreover, there is a satisfactory correspondence with the relative order and trends for the HOMO levels, as mentioned earlier. It is also notable that only one minimum is found for the dichloro derivative with the 6-31 G* method, and this minimum is the *closed* structure. Such a result is also in accord with our qualitative explanation based primarily on the competition between purely bonding and intramolecular steric effects for the dichloro derivative.

The semiempirical and ab initio results for the dimethyl derivative deviate most from experiment. The AM 1 and 3-21 G(*) calculations result in two minima with either a short or long C1–C6 distance. The 6-31 G* calculations converge only at the *closed* structure with an optimized C1–C6 distance of 1.557 Å, which is clearly inconsistent with the crystal structure.[15a] In light of the carefully analyzed experimental data,[15a] computational evaluation of this molecule at higher levels of theory,[41] perhaps with the inclusion of electron configuration interactions (CI) or electron correlation, is necessary. However, because of

their high computation-time requirements, such investigations[42] are only in preliminary stages at this time.

Tables 1 and 2 also list the computational results for other known and unknown compounds with apical π-acceptor or π-donor C11 substituents, as well as calculations relative to the parent CH_2 derivatives. As mentioned earlier, the parent derivatives are reportedly characterized by a conformational equilibrium.[7, 13] Thus, it is not surprising that the energy difference between the two minima is small, and that a low interconversion activation energy of about 5 kcal mol^{-1} for the *closed* structure has been found. In the absence of steric effects and the π-donor/acceptor features of the substituents, the experimental and computational preference for the *open* structure may depend on a subtle energetic interplay within the frontier MOs. Such an effect is difficult to trace at our qualitative interpretational level or from our quantitative results concerning stable minima.

Substituents such as ethynyl, vinyl, and nitro can definitely be assigned π-acceptor character, and they are calculated to result in structures of the *closed* tricyclic type. In addition, ethynyl and vinyl may also exhibit some steric resistance towards transformation to the *open* structure. The slight preference of the disilyl derivative for the *closed* structure is also understandable in terms of steric hindrance (the interconversion activation energy also appears to be higher).

We conclude this section with some comments on the TS structure stationary points (species calculated to exhibit exactly one imaginary frequency), as calculated by the semiempirical AM1 method. Since the AM1 computational method has been parameterized on the basis of experimental structures and properties of ground-state molecules,[19] the extension of such a method to transition-state structures might be questioned. However, in each TS structure, the single imaginary frequency corresponded to a vibrational mode in which the C1—C6 vector lengthened and shortened, as would be expected along a pathway in which the *closed* tricyclic derivative is converted into the *open* bicyclic derivative or vice versa. Further, as discussed elsewhere, the TS structures corresponded closely to the postulated intermediate structure along the EHMO pathway. Thus, even with the caveat concerning the parameterization of the AM1 method, these TS structures appear to be reasonable.

With regard to the geometrical features of the TSs, the structures have nearly exact C_{2v} symmetry even though they were calculated without imposition of any symmetry constraints. Further, when compared to our interconversion pathway, the structures fit closely to points along the pathway we have defined (see VI – VIII). For example, the TS of the dicyano derivative corresponds to the pathway point defined by the values $\Phi = 170$ and $\alpha = 41°$. These two parameters are fundamental geometric features of the rearrangement and, in the transition state, they are almost intermediate between the *closed* ($\Phi = 180$, $\alpha = 25°$) and the *open* ($\Phi = 160$, $\alpha = 51°$) structures. Thus, activation in either the *closed* or the *open* direction appears to require synchronous change in both of these deformations. Finally, the range of activation energy values (5–12 kcal mol^{-1}) suggests that all of the interconversions could occur at ambient temperatures (at least in the gas phase, as these calculations were carried out without any "solvent" parameters).

Conclusions and Extensions

The tautomerism between dinorcaradiene and 1,6-methano-[10]annulene has been newly explored by a synoptic, interpretationally based MO approach, with support from higher-level semiempirical and ab initio calculations. Substituent effects for both known and as-yet-unsynthesized derivatives have been evaluated by using the CACAO graphical interface,[23] which helped to highlight fundamental features of the chemical bonding and its evolution during the interconversion process. The relationship between purely bonding interactions and intramolecular through-space (steric) repulsions establishes a subtle electronic balance between the species during their interconversion along a C_{2v} least-motion pathway.

In the case of the dimethyl derivative, the 6-31 G* ab initio method appears unable to reproduce the experimental features of the molecule, such as the atypical C1—C6 bond length of about 1.8 Å. Future computational work may require higher levels of theory and the incorporation of CI and electron correlation methodologies. Interestingly, the EHMO approach satisfactorily reproduces the geometric features of the dimethyl derivative and, more importantly, highlights a result of chemical significance: the competition for the atomic orbitals on C1 and C6, which can either form a direct C1—C6 σ bond or can π bond with the lateral butadienic wings. The involvement of these orbitals in either σ or π bonding depends on several factors, but even at the long C1—C6 distances (>2.0 Å) observed in the *open* structures, significant σ bonding still exists between these two atoms.

Extensions of this investigation, both in experimental and computational fields, arise from the application of the isolobal concept.[11] As mentioned earlier, there are several examples in the chemistry of C_{60} in which a "handle" on a 6,6-fusion edge is produced through the addition of a d^{10} L_2M or a d^8 L_4M fragment.[11] To the best of our knowledge, an analogous addition has not been reported for naphthalene, nor is any olefin-type transition metal coordination chemistry known for the 6,6-ring fusion edge in naphthalene. In this light, we have performed some preliminary calculations[43] on species such as [(PR$_3$)$_2$M(η^2-(C9,C10)-C$_{10}$H$_8$)] (M = Ni,Pd,Pt) to determine whether such compounds are stable and whether they adopt the *open* or *closed* structure. As expected, the isolobal analogy works well in this instance, and there are indications that the *closed* structure **XXII** is preferred over the *open* structure **XXIII**.

Experimentally, we have also begun to test possible synthetic routes to these organometallic compounds. The direct route involving naphthalene does not seem practical, probably because the deformation from planarity is unfavorable. It may be possible to follow a similar strategy to that of Vogel[1] to obtain the dinorcaradiene and 1,6-methano[10]annulene tautomers; that is, the coordination of a metal species to the central olefin bond of 1,4,5,8-tetrahydronaphthalene (isotetralin), followed by gentle dihydrogenation, and work in this direction is underway.
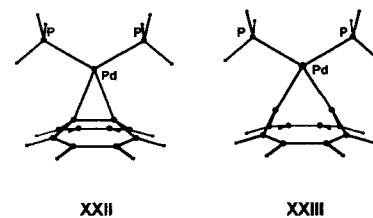
Computational Methods

The semiempirical and ab initio calculations were carried out with the SPAR-TAN[22] suite of programs, running on Silicon Graphics Indigo and Indigo² workstations. In each case, the molecule under consideration was constructed and minimized by using the SPARTAN EXPERT builder mode, which allowed the initial geometry to be either the closed tricyclic dinorcaradiene or the open bicyclic 1,6-methano[10]annulene structure. Following the EXPERT construction and minimization, the EXPERT structure was used as input for a full geometry optimization by the semiempirical AM1 method.[19] The results from the AM1 calculation were then used as the input for full geometry optimization by the ab initio STO-3G method[44] (not reported here), and the geometry which resulted was used as input for full geometry optimization under the 3-21 G(*) methodology.[20] Finally, this latter output was used as input for a full geometry optimization by the 6-31 G* method.[21] Calculations carried out under the imposition of symmetry constraints were accomplished similarly.

Frequency analyses were carried out on all AM1-, 3-21G(*)-, and 6-31 G*-optimized molecules to determine the nature of the stationary points found. All reported transition states resulted in exactly one imaginary frequency, while all molecules reported as minima resulted in all real frequencies, with exactly zero imaginary frequencies.

All of the MO calculations were of the extended Hückel type[18] and used a weighted-modified version of the Wolfsberg–Helmholz formula[45] and standard atomic parameters for the species H, C, N, and O;[18a] F;[46] Si;[47] Cl;[48] and Pd.[49] The three-dimensional drawings and correlation diagrams were performed with the program CACAO.[23] The molecular geometries, based on experimental structures, were parametrized as discussed in the text.

[1] E. Vogel, H. D. Roth, *Angew. Chem. Int. Ed. Engl.* **1964**, *3*, 228.

[2] a) R. V. Williams, H. A. Kurtz, B. Farley, *Tetrahedron* **1988**, *44*, 7455; b) R. C. Haddon, K. Raghavachari, *J. Am. Chem. Soc.* **1985**, *107*, 289; c) L. Farnell, L. Radom, *ibid.* **1982**, *104*, 7650; d) D. Cremer, B. Dick, *Angew. Chem. Int. Ed. Engl.* **1982**, *21*, 865; e) M. J. S. Dewar, M. L. McKee, *Pure Appl. Chem.* **1980**, *52*, 1431; f) A. Gavezzotti, M. Simonetta, *Helv. Chim. Acta* **1976**, *59*, 2984.

[3] a) E. Vogel, W. Klug, A. Breuer, *Org. Synth.* **1974**, *45*, 11; b) E. Vogel, *Pure Appl. Chem.* **1969**, *20*, 237; c) V. Rautenstrauch, H. J. Scholl, E. Vogel, *Angew. Chem. Int. Ed. Engl.* **1968**, *7*, 288; d) E. Vogel, W. A. Böll, *ibid.* **1964**, *3*, 642.

[4] a) W. R. Roth, F. G. Klärner, G. Siepert, H. W. Lennartz, *Chem. Ber.* **1992**, *125*, 217; b) R. R. Andréa, H. Cerfontain, H. J. A. Lambrechts, J. N. Louwen, A. Oskam, *J. Am. Chem. Soc.* **1984**, *106*, 2531; c) B. Briat, D. A. Schooley, R. Records, E. Bunnenberg, C. Djerassi, E. Vogel, *ibid.* **1968**, *90*, 4691.

[5] a) D. G. Barrett, G.-B. Liang, D. T. McQuade, J. M. Desper, K. D. Schladetzky, S. H. Gellman, *J. Am. Chem. Soc.* **1994**, *116*, 10525; b) D. G. Barrett, S. H. Gellman, *ibid.* **1993**, *115*, 9343; c) D. G. Barrett, G. B. Liang, S. H. Gellman, *ibid.* **1992**, *114*, 6915.

[6] a) Y. F. Oprunenko, M. D. Reshetova, S. G. Malyugina, Y. A. Ustynyuk, N. A. Ustynyuk, A. S. Batsanov, A. I. Yanovsky, Y. T. Struchkov, *Organometallics* **1994**, *13*, 2284; b) R. Neidlein, U. Kux, *Angew. Chem. Int. Ed. Engl.* **1993**, *32*, 1324.

[7] P. M. Warner, *J. Am. Chem. Soc.* **1994**, *116*, 11059.

[8] a) T. Ishida, T. Furudate, T. Nogami, M. Kubota, T. Hirano, M. Ohashi, *Fullerene Sci. Tech.* **1995**, *3*, 399; b) A. Hirsch, *Synthesis* **1995**, 895; c) M. Tsuda, T. Ishida, T. Nogami, S. Kurono, M. Ohashi, *Tetrahedron Lett.* **1993**, *34*, 6911.

[9] a) M. Prato, V. Lucchini, M. Maggini, E. Stimpfl, G. Scorrano, M. Eiermann, T. Suzuki, F. Wudl, *J. Am. Chem. Soc.* **1993**, *115*, 8479; b) A. B. Smith III, R. M. Strongin, L. Brard, G. T. Furst, W. J. Romanow, *J. Am. Chem. Soc.* **1993**, *115*, 5829; c) L. Isaacs, A. Wehrsig, F. Diederich, *Helv. Chim. Acta* **1993**, *76*, 1231; d) M. Prato, Q. C. Li, F. Wudl, *J. Am. Chem. Soc.* **1993**, *115*, 1148.

[10] For example: a) [(η²-C₆₀)bis(triphenylphosphane)palladium(o)], V. V. Bashilov, P. V. Petrovskii, V. I. Sokolov, S. V. Lindeman, I. A. Guzey, Y. T. Struchkov, *Organometallics* **1993**, *12*, 991; b) [(η²-C₆₀)bis(triphenylphosphane)platinum(o)], P. J. Fagan, J. C. Calabrese, B. Malone, *Science* **1991**, *252*, 1160.

[11] R. Hoffmann, *Angew. Chem. Int. Ed. Engl.* **1982**, *21*, 711.

[12] J. A. López, C. Mealli, *J. Organomet. Chem.* **1994**, *478*, 161.

[13] G. R. Stevenson, S. S. Zigler, *J. Phys. Chem.* **1983**, *87*, 895.

[14] 1,6-methano[10]annulenes: a) 11,11-(H)₂-, R. Bianchi, T. Pilati, M. Simonetta, *Acta Crystallogr. Sect. B* **1980**, *36*, 3146; b) 11,11-(F)₂-, T. Pilati, M. Simonetta, *Acta Crystallogr. Sect. B* **1976**, *32*, 1912, and C. M. Gramaccioli, M. Simonetta, *ibid.* **1971**, *27*, 2231; c) 11-H-11-C(=O)OH-, ref. [5b]; d) 11-(=O)-, S. Ito, Y. Fukazawa, *Tetrahedron Lett.* **1974**, 1045.

[15] Dinorcaradienes: a) 11,11-(CH₃)₂-, R. Bianchi, G. Morosi, A. Mugnoli, M. Simonetta, *Acta Crystallogr. Sect. B* **1973**, *29*, 1196 and R. Bianchi, A. Mugnoli, M. Simonetta, *J. Chem. Soc. Chem. Commun.* **1972**, 1073; b) 11-CH₃-11-CN-, R. Bianchi, T. Pilati, M. Simonetta, *J. Am. Chem. Soc.* **1981**, *103*, 6426 and R. Bianchi, T. Pilati, M. Simonetta, *Acta Crystallogr. Sect. B* **1978**, *34*, 2157; c) 11,11-(CN)₂-, R. Bianchi, T. Pilati, M. Simonetta, *Helv. Chim. Acta* **1984**, *67*, 1707 and R. Bianchi, T. Pilati, M. Simonetta, *Acta Crystallogr. Sect. C (Crystal Struct. Commun.)* **1983**, *39*, 378 and E. Vogel, T. Scholl, J. Lex, G. Hohlneicher, *Angew. Chem. Int. Ed. Engl.* **1982**, *21*, 869.

[16] H. B. Bürgi, E. Shefter, J. D. Dunitz, *Tetrahedron*, **1975**, *31*, 3089.

[17] H. B. Bürgi, J. D. Dunitz, J. M. Lehn, G. Wipff, *Tetrahedron*, **1974**, *30*, 1563.

[18] a) R. Hoffmann, *J. Chem. Phys.* **1963**, *39*, 1397; b) R. Hoffmann, W. N. Lipscomb, *ibid.* **1962**, *36*, 2872; c) R. Hoffmann, W. N. Lipscomb, *ibid.* **1962**, *36*, 2179.

[19] a) M. J. S. Dewar, C. H. Reynolds, *J. Comp. Chem.* **1986**, *2*, 140; b) M. J. S. Dewar, E. G. Zoebisch, E. F. Healy, *J. Am. Chem. Soc.* **1985**, *107*, 3902.

[20] a) W. J. Pietro, M. M. Franci, W. J. Hehre, D. J. Defrees, J. A. Pople, J. S. Binkley, *J. Am. Chem. Soc.* **1982**, *104*, 5039; W. J. Pietro, M. M. Franci, W. J. Hehre, J. A. Pople, J. S. Binkley, *ibid.* **1982**, *104*, 5048; b) M. S. Gordon, J. S. Binkley, J. A. Pople, W. J. Pietro, W. J. Hehre, *ibid.* **1982**, *104*, 2797; c) J. S. Binkley, J. A. Pople, W. J. Hehre, *ibid.* **1980**, *102*, 939.

[21] a) M. S. Gordon, *Chem. Phys. Lett.* **1980**, *76*, 163; b) P. C. Hariharan, J. A. Pople, *Mol. Phys.* **1974**, *27*, 209; c) P. C. Hariharan, J. A. Pople, *Theor. Chim. Acta* **1973**, *28*, 213; d) W. J. Hehre, R. Ditchfield, J. A. Pople, *J. Chem. Phys.* **1972**, *56*, 2257; e) R. Ditchfield, W. J. Hehre, J. A. Pople, *ibid.* **1971**, *54*, 724.

[22] SPARTAN version 4, Wavefunction, 18401 Von Karman Avenue, Suite 370, Irvine, CA 92715 (USA).

[23] C. Mealli, D. M. Proserpio, *J. Chem. Educ.* **1990**, *67*, 399.

[24] A similar deconstructive/constructive methodology was used to investigate the bonding in bimetallic organometallic systems which contain the anionic indenyl ligand: C. Bonifaci, A. Ceccon, S. Santi, C. Mealli, R. W. Zoellner, *Inorg. Chim. Acta* **1995**, *240*, 541.

[25] Cambridge Structural Database System, version 5.11, Cambridge Crystallographic Data Centre, 12 Union Road, Cambridge, CB2 1EZ (UK)

[26] F. H. Allen, *Acta Crystallogr. Sect. B* **1980**, *36*, 81.

[27] a) R. Hoffman, R. B. Davidson, *J. Am. Chem. Soc.* **1971**, *93*, 5699; b) R. Hoffmann, *Proc. Int. Conf. Pure Appl. Chem.* **1971**, *23*, 233; c) R. Hoffmann, *Tetrahedron Lett.* **1970**, 2907.

[28] a) H. N. C. Wong, M. Hon, C. Tse, Y. Yip, J. M. Tanko, T. Hudlicky, *Chem. Rev.* **1989**, *89*, 156; b) H. Reissig in *The Chemistry of the Cyclopropane Group* (Ed.: Z. Rappoport), Wiley, New York, **1987**, part 1, pp. 375–443.

[29] The concept of σ aromaticity in cyclopropane [30] has been challenged on the basis of results from spin-coupled (SC) theory: P. B. Karadakov, J. Garratt, D. L. Cooper, M. Raimondi, *J. Am. Chem. Soc.* **1994**, *116*, 7714. Their calculated SC theoretical description of cyclopropane does not involve any significant resonance, and they found no evidence in favor of σ aromaticity. However, the SC result has no direct consequences that affect the conclusions reported herein.

[30] a) D. Cremer, J. Gauss, *J. Am. Chem. Soc.* **1986**, *108*, 7467; b) M. J. S. Dewar, *ibid.* **1984**, *106*, 669.

[31] The CACAO input file which generates the Walsh diagram for the described interconversion process can be obtained from one of the authors (C. M.) upon request (mealli@cacao.issecc.fi.cnr.it).

[32] With reference to Figures 2 and 3, these levels can be identified with $1b_{1u} \rightarrow 1a_1$, $1b_{2g} \rightarrow 1b_1$, $1a_u \rightarrow 1a_2$, and the often-illustrated $2b_2$.

[33] a) C. Mealli, J. A. Lopez, M. J. Calhorda, C. C. Romão, W. A. Herrmann, *Inorg. Chem.* **1994**, *33*, 1139; b) C. Mealli, M. Sabat, L. Marzilli, *J. Am. Chem. Soc.* **1987**, *109*, 1593.

[34] J. Osterodt, F. Vögtle, *Chem. Commun.* **1996**, 547.

[35] a) R. F. Childs, *Acc. Chem. Res.* **1984**, *17*, 347; b) L. A. Paquette, *Angew. Chem. Int. Ed. Engl.* **1978**, *17*, 106.

[36] R. Breslow, *Acc. Chem. Res.* **1973**, *6*, 393.

[37] F. Dietz, N. Tyutyulkov, M. Rabinovitz, *J. Chem. Soc. Perkin Trans. 2* **1993**, 157.

[38] a) G. Maier, *Angew. Chem. Int. Ed. Engl.* **1988**, *27*, 309; b) G. Maier, W. Mayer, C. Haacke, R. Askani, *ibid.* **1973**, *12*, 1016; c) O. L. Chapman, C. L. McIntosh, J. Pacansky, *J. Am. Chem. Soc.* **1973**, *95*, 614; d) G. Maier, U. Mende, *Tetrahedron Lett.* **1969**, 3155.

[39] a) L. A. Paquette, *Tetrahedron* **1975**, *31*, 2855; b) O. Bastiansen, L. Hedberg, K. Hedberg, *J. Chem. Phys.* **1957**, *27*, 1311.

[40] C. Mealli, A. Ienco, E. Perez-Correño, P. Paoli, M. Barzaghi, A. Tamulis, *Chem. Eur. J.*, submitted for publication in ....

[41] W. T. Borden, E. R. Davidson, *Acc. Chem. Res.* **1996**, *29*, 67.

[42] C. Mealli, R. W. Zoellner, unpublished results.

[43] C. Mealli, E. B. Hoyt, Jr., R. W. Zoellner, *Third Italian–Israeli Meeting on Chemical Crystallography: "Crystal Structure and Molecular Recognition"*, Ferrara, Italy, February **1996**, pp. 30–32.

[44] a) J. B. Collins, P. von R. Schleyer, J. S. Binkley, J. A. Pople, *J. Chem. Phys.* **1976**, *64*, 5142; b) W. J. Hehre, R. F. Stewart, J. A. Pople, *J. Chem. Phys.* **1969**, *51*, 2657.

[45] J. H. Ammeter, H. B. Bürgi, J. C. Thibeault, R. Hoffmann, *J. Am. Chem. Soc.* **1978**, *100*, 3686.

[46] A. B. Anderson, R. Hoffmann, *J. Chem. Phys.* **1974**, *60*, 4271.

[47] N. Trong Anh, M. Elian, R. Hoffmann, *J. Am. Chem. Soc.* **1978**, *100*, 110.

[48] R. H. Summerville, R. Hoffmann, *J. Am. Chem. Soc.* **1976**, *98*, 7240.

[49] K. Tatsumi, R. Hoffmann, A. Yamamoto, J. K. Stille, *Bull. Chem. Soc. Japan* **1981**, *54*, 1857.